Submitted to Advances in Structural Engineering in July 2012

Experimental Study of Moderately Reinforced Concrete Beams Strengthened with Bolted-Side Steel Plates

L.Z. Li[1], S.H. Lo[2] and R.K.L. Su[3*]

[1] PhD Candidate

[2] Professor

[3] Associate Professor

*Corresponding author

Address: Department of Civil Engineering, the University of Hong Kong, Pokfulam Road, Hong Kong, PRC

Fax number: (852) 2559 5337

Tel. number: (852) 2859 2648

E-mail address: klsu@hkucc.hku.hk

Abstract

Existing reinforced concrete (RC) beams can be effectively strengthened by attaching steel plates to the side faces of the beams using anchor bolts. The performance of this type of beam, bolted side-plated (BSP) beams, is mainly controlled by the degree of partial interaction at the steel-concrete interface. In this study, a total of seven moderately reinforced BSP beams with different steel plate depths and various bolt spacings were tested. Their behaviours were compared to the available test results for lightly reinforced BSP beams obtained by other researchers. The results show that moderately reinforced RC beams are more effective in increasing the flexural strength and ductility capacity using deeper steel plates than the use of a greater number of anchor bolts. It was also found that the longitudinal and transverse slips were controlled by both the stiffness ratios of the steel plates to the RC beam and the force-slip response of the anchor bolts.

Keywords:

Moderately Reinforced Concrete Beam; Strengthening; Bolted Side-Plated Beam; Partial-Interaction; Longitudinal Slip; Transverse Slip; Strain Factor; Curvature Factor

1 INTRODUCTION

Beams in existing reinforced concrete (RC) buildings often need to be strengthened due to material deterioration such as concrete carbonation or steel corrosion as well as the change in usage or compliance with updated design codes. There are several methods available to enhance RC beams, including (1) shortening the length of span by installing additional supports, (2) increasing the cross section area by adding newly cast concrete with reinforcement, and (3) enhancing the cross section by attaching steel plates or fibre reinforced polymers (FRP) to the soffit face or the side faces. The utilisation of the first two methods is very limited because they either shorten the clear span or occupy extra space under the beams and require exhausting labour. In contrast, the latter method has been accepted worldwide over the past several decades for its small space occupancy and execution convenience.

Steel plates attached to RC beams by adhesive bonding usually suffer from serious debonding and peeling (Sharif *et al.* 1995; Adhikary *et al.* 2000; Buyukozturk *et al.* 2004). To overcome these shortcomings, steel plates may be anchored to RC beams by mechanical expansion anchor bolts and chemical anchor bolts to avoid debonding (Roberts and Haji-Kazemi 1989; Su and Zhu 2005). Although attaching steel plates or channels to the beam soffit by anchor bolts can effectively increase the flexural strength and stiffness, it may lead to over reinforcement and shear failure and decrease the ductility of the strengthened beams as a consequence (Roberts and Haji-Kazemi 1989; Foley and Buckhouse 1999). Su and Zhu (2005) therefore proposed to attach steel plates to the beam side faces using anchor bolts. RC beams strengthened by this technique, bolted side-plated (BSP) beams, have proven to be significantly enhanced in terms of flexural strength without a visible decrease in the ductility.

Unlike RC beams strengthened with steel plates on the beam soffit, in which only longitudinal slip exists, both longitudinal and transverse slips coexist on the steel-concrete interface in BSP beams, as illustrated in Figure 1. The degree of partial interaction between the bolted-side plates and the RC beams, which controls the behaviours of the BSP beams, is affected by the longitudinal and transverse

slips. Its effect can be quantified by two indicators, the strain factor and the curvature factor (Siu 2009). As illustrated in Figure 2, the strain factor α_ε is defined as the longitudinal strain ratio between the steel plates and the RC beam at the centroidal level of the steel plates and is used to denote the axial strain looseness of the steel plates due to the longitudinal slip; the curvature factor α_φ is defined as the curvature ratio between the steel plates and the RC beam and is used to denote the curvature reduction of the steel plates due to the transverse slip.

Various theoretical and experimental studies have been conducted all over the world to study the performance of BSP beams. Oehlers et al. (1997) established the relationship between the degree of transverse-partial-interaction and the properties of anchor bolts, but the uniform shear distribution assumption on the steel-concrete interface is hard to justify in many real applications. Based on this model, Nguyen et al. (2001) derived the relationship between longitudinal and transverse partial interactions as well as the distribution of slip strain, slip and neutral-axis-separation; however, the assumption of a single curvature for both the steel plates and the RC beam in the calculation of the neutral-axis-separation violates the transverse-partial-interaction condition. Su and Zhu (2005) conducted experimental and numerical studies on BSP coupling beams and showed that small slips on the steel-concrete interface could significantly affect the overall response of BSP beams. Su and Siu proposed some numerical procedures for predicting the nonlinear load-deformation response of bolt groups (Su and Siu 2007; Siu and Su 2009) as well as the longitudinal and transverse slip profiles (Siu 2009; Siu and Su 2011) in BSP beams. Their predicted longitudinal slips were in good agreement with the test results obtained at some discrete locations on the beams (Siu and Su 2010). However, the complete longitudinal and transverse slip profiles along the entire BSP beam were not measured.

The structural behaviours of RC beams are controlled by the steel ratios of tensile reinforcement and can be classified by the balanced steel ratio ρ_{stb}, at which the yielding of the outermost tensile-reinforcement-layer and the crushing of concrete occur simultaneously. If an RC beam is lightly reinforced with a tension steel ratio of $\rho_{st} < \rho_{stb}$, it will fail in a ductile mode, and both its strength and stiffness can be increased significantly by adding external reinforcement with a small sacrifice of

ductility. In contrast, if an RC beam is over-reinforced with $\rho_{st} > \rho_{stb}$, its strength and stiffness are controlled by the compressive strength of the concrete rather than the strength of the tensile reinforcement, and adding external tensile reinforcement will cause the beam to fail in a brittle mode with very little ductility. It is noted that over-reinforced RC beams are forbidden for use in structural design, and a strengthening design for this type of beam is rarely needed. However, there is a large number of moderately reinforced RC beams in existing building stock whose tensile steel ratios are lower than but very close to ρ_{stb}. It is not appropriate to strengthen these beams by simply adding steel plates or FRPs onto the tension sides of the beam because it would lead to over-reinforcement problems.

Most of the available strengthening techniques up to now have focused on lightly reinforced RC beams. Roberts et al. (1989) proposed a method to strengthen under-reinforced RC beams with a ρ_{stb} of 1.21% by bolting steel plates to the beam soffit, Foley et al. (1999) proposed a technique by bolting steel channels to the tension face of the lightly reinforced RC beams with a ρ_{st} of 0.54%, Ruiz et al. (1999) studied the size effect and bond-slip dependence of lightly reinforced RC beams with a ρ_{st} less than 0.3%, and Siu and Su (2011) studied the partial interaction of lightly reinforced BSP beams with a ρ_{st} of 0.85%.

In light of this situation, an improved strengthening technique is proposed for moderately reinforced RC beams in this study. Instead of attaching steel plates to the beam soffit or shallow steel plates to the tensile region of the side faces, deep steel plates extending from the tensile region to the compressive region were attached to the side faces of the beam by anchor bolts. Compared with the first two methods, using deep steel plates could increase not only the tensile reinforcement, thus enhancing the flexural strength and stiffness, but also the compressive reinforcement, thus reducing the degree of reinforcement and upgrading the ductility. However, as a result of using deep steel plates, detrimental plate buckling, which might occur in the compressive regions of the steel plates, should be suppressed by stiffeners. In this study, an experimental study was conducted to investigate the strengthening effects of this method, to quantify the partial interaction and to measure the complete longitudinal and

transverse slip profiles in BSP beams. The test results were compared with those of the lightly reinforced BSP beams tested previously (Siu 2009; Siu and Su 2011; Su *et al.* 2010).

2 EXPERIMENTAL STUDY

2.1 Specimen details

To compare with the lightly reinforced RC beams tested by Siu (2009), a total of seven RC beams with the same properties but different tensile steel ratios were fabricated and tested. The length of the beams was 4000 mm, and the cross section was 225 mm × 350 mm. The reinforcement details of the specimens are shown in Figure 3. Compressive reinforcement of 2T10 and transverse reinforcement of R10-100 were used for all specimens. The notations ‘T’ and ‘R’ denote the high-yield deformed steel bars and the mild steel round bars, respectively. Tensile reinforcement of 3T16, which is the same as those adopted by Siu (2009), was chosen for Specimen P75B300, and 6T16 was used for the rest of the specimens. The corresponding tensile reinforcement ratios were 0.85% and 1.77%, respectively.

A control RC beam, namely, CONTROL, without any retrofitting measures was used as a reference to demonstrate the beam performance before strengthening. The other specimens were strengthened with two steel plates anchored to their side faces and were named according to the design parameters, such as the depth of steel plate and the horizontal bolt spacing, which have primary effects on strengthening. Table 1 summarises the names of the specimens and the design parameters of the steel plate, anchor bolt and buckling restraint arrangements for all the specimens. To show the difference in responses between the lightly and moderately reinforced BSP beams clearly, the results of tests on three lightly reinforced BSP beams conducted by Siu (2009), CONTROL*, P75B300*, P150B400*, were also extracted for comparison. The design parameters of these lightly reinforced PSB beams are also listed in Table 1.

Figures 4 and 5 show the section views and the elevations of the steel plate and anchor bolt arrangements for all of the specimens. Steel plates with a thickness of 6 mm and a length of 3950 mm were used for all BSP specimens. Three different plate depths, 75 mm, 100 mm and 250 mm, were

chosen to yield distinct strengthening effects. For Specimen P75B300, two steel plates with a depth of 75 mm were fixed onto the side faces by ten bolts located at the centroidal level of the plates with a horizontal bolt spacing of 300 mm. All bolts were assigned to the shear span, and none were located in the pure bending zone following the arrangements of the lightly reinforced BSP beams proposed by Siu (2009). For Specimens P100B250 and P100B450, two shallow steel plates with a depth of 100 mm were installed by a row of anchor bolts with a uniform spacing of 300 mm and 450 mm, respectively. For Specimens P250B300, P250B300R and P250B450R, two deep steel plates with a depth of 250 mm were fixed by two rows of anchor bolts with a horizontal spacing of either 300 mm or 450 mm. To study the influence of plate buckling, which might occur in the compressive zones of the steel plates, buckling restraint devices were introduced to Specimens P250B300R and P250B450R but not to Specimen P250B300.

2.2 Strengthening procedure

The anchor bolt installation procedure followed the instructions in the technology manual provided by Hilti Corporation (2011). Strengthening measures were conducted three weeks after the RC beams were cast. Drilled holes with a diameter of 12 mm and a depth of 105 mm were formed using a rotary hammer on the side faces and cleaned thoroughly. HIT-RE 500 adhesive mortar was then injected into the holes, and HAS-E anchor rods with a diameter of 10 mm were turned into the mortar until they reached the required depth of 95 mm.

Drilled holes with a diameter of 12 mm were also formed in the steel plates. After the adhesive mortar in the RC beams was cured, the steel plates were fixed to the side faces of the beam. The HIT-RE 500 adhesive mortar was also injected into the clearances between the anchor rods and the steel plates using dynamic sets for all specimens except Specimen P75B300 to study the effects of slips at the rod-plate clearances. A dynamic set, as shown in Figure 6, was composed of an injection washer used to inject adhesive mortar, a spherical washer designed to prevent the mortar from leaking and an ordinary nut to fix the steel plates and the washers on the concrete surface.

The buckling restraint device shown in Figure 7 was composed of steel angles L63 × 5 mm, which were used to prevent the steel plates from buckling. Steel plates with a thickness of 10 mm were installed at the top row of anchor bolts to fix the steel angles. To avoid adding extra strength and stiffness to the BSP beams, the steel angles were connected to the thick steel plates by bolt connections with slotted holes, which allow the steel angles to rotate and move in the longitudinal direction. The interface between the steel angle and the thick steel plate was carefully sanded and lubricated to diminish any possible friction.

2.3 Material properties and bolt test

The concrete mix proportion adopted in this study is tabulated in Table 2. The mix used 10 mm coarse aggregate with a water-to-cement ratio of 0.72, an aggregate-to-cement ratio of 6.68 by weight, and a measured slump of 50 mm. For each specimen, four 150 mm × 150 mm × 150 mm concrete cubes and four Ø150 mm × 300 mm cylinders were cast, and compressive tests were performed on the test day to obtain the compressive strengths, which are listed in Table 1.

High-yield deformed steel bars (T) were used for compressive and tensile reinforcement while mild steel round bars (R) were used for transverse reinforcement. Three bar samples with a length of 500 mm were taken from each type of reinforcement for tensile tests to obtain the yield strength and Young's modulus. The side plates were made of mild steel. Three 500 mm × 50 mm strips were used for tensile tests to determine the yield strength and Young's modulus of the steel plates. The material properties of the reinforcement and the steel plates are tabulated in Table 3.

The "HIT-RE 500 + HAS-E" chemical anchoring system (Hilti Corporation 2011), which was provided by Hilti Corporation, was chosen as the connecting media between the steel plates and the RC beams. The HAS-E anchor rods were Grade 5.8 and covered by a galvanised surface with a thickness of at least 5 μm. The HIT-RE 500 adhesive mortar was a two-component, ready mix epoxy resin, and its working and curing time were 30 minutes and 12 hours, respectively, at a base-material temperature of 20 °C.

To determine the load-slip response of the “HIT-RE 500 + HAS-E” anchoring system, three RC blocks with the same sectional properties as the RC beams and with a length of 200 mm were cast and fabricated. Holes were drilled, and bolts were planted with HIT-RE adhesive mortar following the aforementioned procedure. A specifically designed transfer plate, as shown in Figure 8, was used to conduct compression shear tests on the anchor rods. The samples were loaded using a hydraulic jack, and a monotonic displacement controlled load was applied to the transfer plate. The two strengthened steel plates, which simulated the bolted-side plates, transferred the compression force to shear forces and applied them to the two anchor bolts. The load increased at a rate of 0.01 mm/sec and terminated when either bolt failed. Figure 9 shows the force-slip responses. The peak bolt force was 53 kN, and the slip at the peak force was 4 mm. The secant modulus at 25% of the peak force, which was chosen to represent the initial elastic stiffness, was 112 kN/mm.

2.4 Test set-up

This experimental study was conducted in a test frame in the Structural Engineering Laboratory at The University of Hong Kong. The clear span between the two roller supports, which were bolted to the strong floor, was 3600 mm. A monotonic load provided by a 500 kN capacity hydraulic jack was equally divided into two concentrated forces by a steel transfer beam and applied at the two trisection points of the specimen under test. Hence, a pure bending zone with a length of 1200 mm was generated in the middle part of the specimen, as illustrated in Figure 10.

To investigate the load-deflection behaviours, especially in the post-peak region, a displacement controlled loading process was designed for the specimens in this study. The loading rate was chosen to be 0.01 mm/sec up to 50% of the theoretical peak load. Then, it was increased to 0.02 mm/sec until the post-peak load decreased to 80% of the actual peak load, and the test was terminated.

2.5 Instrumentation

The longitudinal tensile and compressive strains in the reinforcement and steel plates were measured

by strain gauges. The shear strains in the steel plates were determined by rosette strain gauges. The arrangement of strain gauges is shown in Figure 11(a).

To measure the deformation of the specimen under testing, LDTs were employed to measure the vertical deflections at several sections along the specimen; four LVDTs were also designed to determine the rotations at both supports, as shown in Figure 11(b). To quantify the relative slips between the steel plates and the RC beam, a slip measuring device was tailor made, as shown in Figure 12. This device was composed of aluminium angles, plates and bolting connectors. It included two sets: Set A was embedded into the RC beam through two expansion bolts, where one was located in the compressive region of the side face and the other was in the beam soffit, and Set B was fixed onto and moved with the steel plate when relative slips occurred. Three LVDTs were installed on Set A. One set was in the transverse direction with the probe tip in contact with the lower edge of the steel plate, and the other two were in the longitudinal direction with the probe tips pointing at the upper and lower sides of Set B. Hence, if slips occurred, the first LVDT measured the transverse slip, and the other two recorded the longitudinal slips. Furthermore, rotational slips could be deduced from the longitudinal slips.

3 EXPERIMENTAL RESULTS AND DISCUSSION

3.1 Failure mode

The macroscopic failure modes of RC beams can be categorised as two primary types: (1) flexural failure preceded by the yielding of the tensile reinforcement, which is common in under-reinforced beams and (2) brittle failure caused by crushing of the concrete, which occurs in over-reinforced beams. For BSP beams, two more failure modes can be found: (3) flexural failure preceded by the yielding of the tensile regions of the steel plates and (4) brittle failure attributed to the buckling of the compressive regions of the steel plates. The microscopic phenomena that initiate the corresponding macroscopic failure modes can be described, respectively, as follows: (1) the strain of the outermost tensile-reinforcement-layer reaches its yield strain $\varepsilon_{st} > \varepsilon_y$, (2) the maximum compressive strain of the

concrete exceeds its crushing strain $\varepsilon_{cc} > \varepsilon_{c0}$, (3) the maximum tensile strain of the steel plates reaches its yield strain $\varepsilon_{pt} > \varepsilon_{py}$, and (4) the maximum compressive strain on the outer face of the steel plates decreases suddenly $\Delta\varepsilon_{pc} < 0$.

To classify the failure modes of the specimens, the order of occurrence of these microscopic phenomena with respect to load levels (F/F_p) are tabulated in Table 4. The load-deflection curves at the mid-span of the specimens are shown in Figure 13.

The failure of Specimen CONTROL for the moderately reinforced reference beam was initiated by the yielding of the tensile reinforcement (at $F/F_p = 0.91$) and followed closely by the crushing of the concrete (at $F/F_p = 0.94$). Figure 13(a) shows that the beam failed in a flexural mode, but its ductility was lower than the lightly reinforced reference beam CONTROL* (Siu 2009) due to the use of more tensile steel.

Figure 13(b) shows that the lightly reinforced BSP beams P75B300* and P150B400* (Siu 2009) failed in very brittle modes compared to CONTROL*. Because there were no anchor bolts assigned to the pure bending zones of these beams, enormous transverse slips occurred after the formation of plastic hinges, as shown in Figure 14. Hence, the effective lever arms provided by the steel plates were seriously reduced, and the load-carrying capacities and stiffness decreased rapidly in the post-peak region producing the steep descending branches. In contrast to the RC beams with steel plates on the beam soffits, for which plate-end anchor bolts are sufficient, the BSP beams require a uniform distribution of anchor bolts over the entire span.

Specimen P75B300 did not suffer from this detrimental effect and behaved in a more ductile manner than its counterpart P75B300*. Its failure was caused by the yielding of the tensile reinforcement (at $F/F_p = 0.77$) because the gaps between the bolt rods and the clearance holes of P75B300 were not filled with adhesive mortar. The slips between the bolt rods and steel plates weakened the connection stiffness and hence the strength contribution from the steel plates and caused substantial reductions of the degree of reinforcement and the flexural strength of the beam.

The failure of both P100B300 and P100B450 was caused by the crushing of the concrete (at

F/F_p = 0.78 and 0.80, respectively). Figure 13(c) shows that their descending branches are shorter and steeper compared to that of Specimen CONTROL. The reason is that the shallow steel plates attached to the tensile region of the RC beams acted as additional tensile reinforcement, which caused over-reinforcement and brittle failure. It is evident from Figures 15(a) and 15(b) that a large portion of concrete was crushed when the steel plates were only slightly deformed for both specimens. These phenomena reveal that attaching shallow steel plates to the beam soffit or the tensile regions at the side faces of the beam is not suitable for moderately reinforced RC beams.

In contrast, the steel plates in P250B300R and P250B450R yielded in tension at a very early loading stage (at F/F_p = 0.44 and 0.29, respectively). Thus, the strength contributions from the steel plates were very high, and if thicker steel plates were used, the strength of these specimens could increase. The yielding of the tensile reinforcement occurred relatively late (both at F/F_p = 0.83) and was followed by the crushing of the concrete (at F/F_p = 0.84 and 0.89, respectively), mainly at the concrete covers, as shown in Figures 15(c) and 15(d). These two specimens failed in flexural modes with very high strengths and deformations. The comparison of their load-deflection curves is presented in Figure 13(c).

The performances of Specimens P250B300 and P250B300R were very similar at the early loading stages, as shown in Figure 13(d). The steel plates of P250B300 yielded in tension at a very early loading stage (when F/F_p = 0.26). The crushing of the concrete (at F/F_p = 0.85) occurred prior to the yielding of the tensile reinforcement (at F/F_p = 0.88). Subsequently, serious buckling occurred on the compressive edges of the steel plates (see Figure 16) before reaching the peak load. The compressive region of the steel plates lost its strength, and the specimen behaved as an over-reinforced RC beam with shallow steel plates attached to its tensile region. The beam then failed rapidly.

3.2 Strength, stiffness and ductility

RC beams in a building are expected to have sufficient strength and stiffness within the intended design life and deform significantly before failure under extreme loads. To compare the strength,

stiffness and ductility of the lightly (Siu 2009) and moderately reinforced BSP beams, an equivalent elasto-plastic system, as shown in Figure 17, is used to represent the simplified load-deflection curves of the specimens. The peak load F_p is chosen as the yield strength. A line starting from the origin, crossing the point on the ascending branch at the load level of 0.75 and terminated at the peak load is defined as the elastic branch, and its slope represents the stiffness of the beam $K_{e.}$ A horizontal line with a capacity equal to F_p is the plastic branch. The point on the descending branch, where the load is equal to $0.8F_p$, is chosen as the end of the plastic branch. Ductility can be quantified by the modulus of toughness U_t (Feng *et al.* 2004), where U_t is the area under the entire load-deflection curve, which represents the amount of energy absorbed before failure.

The primary parameters ($F_{p,}$ $K_{e,}$ U_t) that indicate the overall behaviours (strength, stiffness and ductility) of the lightly and moderately reinforced BSP beams are tabulated and compared with the reference RC beams in Table 5. The numbers preceding the parentheses are the absolute values of the parameters, while those inside the parentheses are the ratios of the parameters relative to those of the corresponding reference beam.

3.2.1 Strength and stiffness

Table 5 shows that the strength and stiffness improvements (1.43 and 1.15, respectively) of P75B300* are higher than those (1.18 and 1.04, respectively) of P100B300, and the improvements (1.59 and 1.34, respectively) of P150B400* are also higher than those (1.43 and 1.26, respectively) of P250B300R. Therefore, the improvements in terms of the strengths and stiffness of all of the lightly reinforced BSP beams are higher than those of the moderately reinforced BSP beams, even with shallower steel plates and fewer anchor bolts. This result shows that it is more difficult to enhance RC beams with a higher degree of reinforcement. However, for the lightly reinforced Specimen P75B300 in this study, these improvements are much lower than those of its counterpart P75B300* due to the delayed response caused by slips at the clearance holes, as mentioned in Section 3.1.

Among the moderately reinforced specimens, the improvements in terms of the strength and

stiffness (1.43 and 1.26, respectively) of P250B300R with a plate depth of 250 mm are much higher than those (1.18 and 1.04, respectively) of P100B300 with a plate depth of 100 mm. In addition, the improvements (1.43 and 1.26, respectively) of P250B300R with a bolt spacing of 300 mm are nearly the same as those (1.41 and 1.27, respectively) of P250B450R with a bolt spacing of 450 mm. Thus, the strength and stiffness improvements increase significantly with the depth of the steel plates but not the bolt spacing. Furthermore, the improvements (1.18 and 1.04, respectively) of P100B300 are even slightly lower than those (1.22 and 1.16, respectively) of P100B450 because these two specimens were over-reinforced by shallow steel plates. The failure was due to the concrete crushing, and their strengths were controlled by the concrete strength. Specimen P100B300 had the lowest concrete cube strength (see Table 1), which resulted in the lowest strength and stiffness among all of the moderately reinforced specimens.

The strength improvement was increased from 1.34 for Specimen P250B300 without plate buckling restraint to 1.43 for Specimen P250B300R with buckling restraint devices. However, the stiffness improvements of these two specimens (1.26 and 1.27, respectively) are almost the same. Hence, the improvement due to the use of buckling restraint devices is significant for the beam strength but not for the stiffness. The reason is that plate buckling usually occurs just before reaching the peak load. It does not affect the stiffness, which is mainly controlled by the elastic behaviour at the initial loading stages.

3.2.2 Ductility and toughness

As mentioned earlier, the modulus of toughness (U_t) can be used to measure the ductility. Table 5 shows that due to the use of uniformly distributed anchor bolts along the entire steel plates, the modulus of toughness of all of the moderately reinforced BSP beams is higher than that of the lightly reinforced BSP beams. For example, the ratio U_t is 0.80 for Specimen P100B300, which is higher than that of 0.64 for Specimen P75B300*, and the value 1.48 of P250B300R is much higher than the value 0.67 of P150B400*. Due to the slips at the clearance holes for Specimen P75B300, its modulus of

toughness ratio 1.39 is much higher than the value 0.64 of its counterpart (Specimen P75B300*).

Among the moderately reinforced BSP beams, the modulus of toughness ratios for specimens with shallow steel plates (Specimens P100B300 and P100B450) are reduced (0.80 and 0.89, respectively) due to the increase in the degrees of reinforcement. Specimen P100B300 had a very low ratio due to the low concrete strength and hence a high degree of reinforcement. On the other hand, the ratios of U_t of the plate buckling restrained Specimens P250B300R and P250B450R are enhanced significantly (1.48 and 1.37, respectively) because the compressive zone of the steel plates significantly reduced the degrees of reinforcement. However, when plate buckling was not restrained, the ratio of U_t dropped from 1.48 for Specimen P250B300R with buckling restraints to 0.66 for Specimen P250B300 without buckling restraints.

3.3 Longitudinal and transverse slips

The longitudinal and transverse slips are attributed to the looseness of the axial strain or the curvature of the steel plates, therefore affecting the behaviour of the BSP beams significantly. The longitudinal slip S_{lc} is controlled by the axial stiffness ratio $\beta_a = (EA)_p / (EA)_c$, the flexural stiffness ratio $\beta_f = (EI)_p / (EI)_c$ and the stiffness of the connecting media k_m. The transverse slip S_{tr} is controlled by the flexural stiffness ratio β_f and the stiffness of the connecting media k_m.

The longitudinal and transverse slip profiles from mid-span to one of the supports of the moderately reinforced BSP beams at four different load levels (F/F_p = 0.25, 0.5, 0.75 and 1) are illustrated in Figures 18 and 19, respectively. The values of those at the supports and the loading points at two load levels (F/F_p = 0.75 and 1) are tabulated in Table 6. Because the longitudinal slip varies along the section depth, the value at the centroidal level of the steel plates is adopted as the nominal longitudinal slip.

3.3.1 Longitudinal slip

It is shown in Figure 18 that the longitudinal slips in all of the BSP beams were initiated at the plate-

ends and spread progressively toward the mid-span region. The longitudinal slips of the specimens with shallow steel plates, Specimens P100B300 and P100B450, decreased from the plate-ends and vanished near the mid-span. In contrast, the longitudinal slips of the specimens with deep steel plates, Specimens P250B300R and P250B450R, were more complicated. The direction of slips in the mid-span region changed alternately because the centroidal level of the steel plates and the neutral axis of RC beams were close to each other, and thus small variations on the neutral axis level led to alternations of the slip direction. The figure also shows that the incremental slip in each load step is approximately double of that in the previous step. Thus, the longitudinal slip is proportional to the square of the load level (F/F_p) because the increase of the axial stiffness ratio β_a caused by the stiffness deterioration of the RC beam was accelerated by the development of concrete cracking and crushing as the load levels increased.

Table 6 shows that for specimens with the same plate depth, the plate-end longitudinal slip (2.67 mm) of P100B450 with a bolt spacing of 450 mm is approximately 1.7 times of that (1.50 mm) of P100B300 with a bolt spacing of 300 mm. The results demonstrate that the longitudinal slip is inversely proportional to the bolt spacing. Specimens P250B300R and P100B300 had the same bolt spacing of 300 mm, and the longitudinal slips (0.29 mm) of P250B300R with deep steel plates was only approximately 1/5 of that (1.50 mm) of P100B300 with shallow steel plates at $F/F_p = 1$. Hence, the longitudinal slip is no longer a dominant factor for evaluating the performance of BSP beams with deep steel plates.

3.3.2 Transverse slip

Figure 19 shows that the transverse slips are close to zero at the mid-span, negative near the plate-ends and positive with a maximum magnitude near the loading points for all BSP beams. Obviously, the transverse slips are caused by the shear force transferred from the RC beams to the steel plates, and the directional reversal reveals the bolt force equilibrium in the transverse direction. The high flexural stiffness ratio (β_f) caused by the serious stiffness deterioration at the plastic hinge regions led the

largest slip to occur near the loading points.

Table 6 shows that for the BSP beams with the same size of steel plates, the transverse slips at the loading points of P100B300 and P100B450 were 0.07 mm and 0.12 mm, respectively, at $F/F_p = 0.75$ but then increased to 0.30 mm and 0.23 mm, respectively, at $F/F_p = 1$. The results imply that the transverse slip increases with the number of anchor bolts when $F/F_p \leq 0.75$, but afterwards it is controlled by the concrete strength. The enormous increase (from 0.07 mm to 0.30 mm) of P100B300 in the load interval $F/F_p = 0.75$~1 was caused by the significant increase in the flexural stiffness ratio (β_f) due to the rapid deterioration of the flexural stiffness of the reinforced concrete component after reaching the peak load. The figures in the table also show that when the BSP beams have the same bolt spacing, the transverse slips increase significantly with the increase in plate depth. As an illustration, the transverse slips at the loading point (0.07 mm and 0.30 mm) of P100B300 are much lower than those (0.17 mm and 0.46 mm) of P250B300R at load levels of both 0.75 and 1.

It can be found by comparing the longitudinal and transverse slips in Table 7 that for the BSP beams with shallow steel plates, the transverse slip is less than 10% of the longitudinal slip; however, for the BSP beams with deep steel plates, the longitudinal and transverse slips are of the same order of magnitude. Hence, the effects of transverse slips on BSP beams with deep steel plates cannot be ignored.

3.4 Strain and curvature factors

The strain and curvature factors can be used to quantify the degrees of the axial strain looseness or the curvature reduction of the steel plates due to the longitudinal or transverse slips. The factors are controlled by the stiffness ratios (β_a and β_f) and the stiffness of the connecting media k_m and decrease as the slips increase. Figure 20 illustrates the variations of the strain and curvature factors against the mid-span deflection together with a comparison to the lightly reinforced BSP beam P75B300*.

3.4.1 Strain factors

As shown in the figure, the strain factors of all of the BSP beams with shallow steel plates were approximately 0.7 at the beginning of the loading process and decreased gradually to approximately 0.3 at the peak load. The strain factors of P75B300* were the highest due to its weakest steel plates and therefore lowest axial stiffness ratio β_a. The strain factors of P100B300 were higher than those of P100B450 as a result of its smaller bolt spacing and hence higher connection stiffness k_m. The strain factors of the two BSP beams with deep plates, P250B300R and P250B450R, were very small because their axial stiffness ratios β_a were high and the centroidal levels of their steel plates and RC beams were close together, resulting in negligible centroidal strains in the steel plates.

3.4.2 Curvature factors

The curvature factors of all of the moderately reinforced BSP beams remained unchanged at a high level of 0.8 over the whole loading process. Furthermore, the curvature factors of the specimens with shallow plates were even higher due to the lower flexural plate stiffness and thus lower flexural stiffness ratio β_f. The curvature factor of P75B300* also remained at a high level at the initial loading stages but decreased significantly after the yielding of the tensile reinforcement as a consequence of the enormous transverse slips caused by the lack of anchor bolts at the mid-span.

3.5 Plate behaviour

The steel plates in BSP beams retrofit the RC beam in two primary ways: (1) behaving as additional tensile reinforcement to apply an eccentric compressive force T_p to the RC beam, thus providing an additional coupling moment $M_{p,t} = T_p e_p$, where e_p is the eccentricity, and (2) resisting the lateral loads due to their flexural stiffness directly and hence providing an additional bending moment $M_{p,b}$. The latter strengthening effect is unique and distinct from that of the steel plates attached to the beam soffit.

The tensile forces and bending moments of the steel plates in the BSP beams with shallow or deep plates at two load levels (F/F_p = 0.75 and 1) are tabulated in Table 7, and their contribution to the

flexural strength of the BSP beams is also compared. The values within the parentheses are the ratio of the tensile force to the yield strength of the steel plates. The steel plates in the BSP beams with shallow plates, P100B300 and P100B450, contributed almost half of their tensile strength. For the BSP beams with deep steel plates, P250B300R and P250B450R, the tensile force was relatively low and was only approximately a quarter of their tensile strength. However, the bending moments of the steel plates in P100B300 and P100B450 were very limited and almost less than 10% of those in P250B300R and P250B450R. The ratio of the flexural contributions of the coupling moment provided by their tensile axial force $T_p e_p$ to the bending moment provided by their flexural stiffness $M_{p,b}$ is tabulated in Table 7. The bending moment $M_{p,b}$ taken by the shallow plates was only 15% of the coupling moment $T_p e_p$, whereas the bending moment $M_{p,b}$ in the deep plates was approximately 7 times of the coupling moment $T_p e_p$.

4 CONCLUSIONS

This paper presented an experimental investigation of the strength, stiffness, ductility, longitudinal and transverse slips, strain and curvature factors as well as the plate behaviour of moderately reinforced BSP beams under four-point bending. The results for the moderately reinforced BSB specimens were compared with the available test results for lightly reinforced BSP beams reported by other researchers. The main findings of this study are summarised as follows:

(1) The experimental results reveal that unlike the lightly reinforced RC beams, whose strength and stiffness can be increased significantly with a small sacrifice of ductility by attaching steel plates to the beam soffit or the tensile region of the side faces, the strength and stiffness of moderately reinforced RC beams are controlled by the concrete strength. The flexural strength can only be improved by adding deep bolted-side steel plates extending to the compressive zones of the beam side faces.

(2) Deep steel plates in BSP beams are prone to buckling on their compressive edge. This phenomenon has serious adverse effects on strength and ductility but not stiffness. Buckling restraints should be added to prevent the plate from buckling and to improve the post-peak performance of the beam.

(3) In contrast to ordinary strengthened RC beams with the steel plates attached to the beam soffit, for which plate-end anchor bolts are sufficient, BSP beams require a uniform distribution of anchor bolts over the entire span; otherwise, enormous transverse slips will occur at mid-span and jeopardise the load-carrying capacity of the beam.

(4) The clearance between the bolt rods and steel plates weakens the connection stiffness and therefore reduces the strength contribution from the steel plates and hence the degree of reinforcement. The reduction of the degree of reinforcement can decrease the strength of the beam and increase the ductility to some extent.

(5) The strengthening effect of BSP beams is affected by the properties of the connecting media and is determined by the bolt spacing and the force-slip response of the anchor bolts.

(6) Longitudinal slip is initiated from the plate-ends and decreases progressively toward the mid-span. In BSP beams with deep steel plates, the longitudinal slips at the centroidal level of the steel plates may reverse in direction alternatively. Longitudinal slips increase with increasing bolt spacing and stiffness ratios of the steel plates to the RC beams.

(7) A transverse slip changes its direction from the plate-ends to the middle pure bending zone, reaches its maximum magnitude near the loading points and decreases to zero at mid-span. Transverse slips increase with the flexural stiffness ratios and hence the plate-depth. They also increase with the bolt spacing before reaching the load level of 0.75, above which they are controlled by the concrete compressive strength.

(8) For BSP beams with shallow steel plates attached to the tensile region of the side faces, longitudinal slips are the dominant factor for evaluating the performance of the beam, and transverse slips can be neglected. However, for BSP beams with deep steel plates, longitudinal slips are no longer a dominant factor, and the transverse slips control the behaviour of the beam.

(9) Both the strain and curvature factors increase with the number of anchor bolts used and the reduction of the stiffness ratios. The strain factors of BSP beams with shallow steel plates decrease gradually from a relatively high level at the early loading stage to a low level at the peak load.

However, those of BSP beams with deep steel plates remain very low over the whole loading process due to the small difference in the centroidal levels of the steel plates and RC beams. The curvature factors remain at a relative high level over the entire loading process.

(10) The steel plates in BSP beams contribute to the overall flexural strength by both the coupling moment provided by their axial tensile forces and the bending moment provided by their flexural stiffness. Shallow steel plates contribute mainly to the former, whereas deep plates contribute mainly to the latter.

ACKNOWLEDGMENTS

The research described here received financial support from the Research Grants Council of the Hong Kong SAR (Project No. HKU7166/08E and HKU715110E) and technical support from the HILTI Corporation, which are gratefully acknowledged.

REFERENCES

Adhikary, B.B., Mutsuyoshi, H., and Sano, M. (2000). "Shear strengthening of reinforced concrete beams using steel plates bonded on beam web: experiments and analysis", *Construction and Building materials*, Vol. 14, No. 5, pp. 237–244.

Buyukozturk, O., Gunes, O., and Karaca, E. (2004). "Progress on understanding debonding problems in reinforced concrete and steel members strengthened using FRP composites", *Construction and Building Materials*, Vol. 18, No. 1, pp. 9–19.

Feng, P., Ye, L., Zhao, H., and Zhuang, J. (2004). "Review and new proposals for performance indices of flexural members", *Proc. 8th International Symposium on Structural Engineering for Young Experts. Science Press*, pp. 121–130.

Foley, C.M. and Buckhouse, E.R. (1999). "Method to increase capacity and stiffness of reinforced concrete beams", *Practice Periodical on Structural Design and Construction*, Vol. 4, No. 1, pp. 36–42.

Hilti Corporation. (2011). *Fastening Technology Manual*, Hong Kong.

Nguyen, N.T., Oehlers, D.J., and Bradford, M.A. (2001). "An analytical model for reinforced concrete beams with bolted side plates accounting for longitudinal and transverse partial interaction", *International Journal of Solids and Structures*, Vol. 38, No. 38-39, pp. 6985–6996.

Oehlers, D.J., Nguyen, N.T., Ahmed, M., and Bradford, M.A. (1997). "Transverse and longitudinal partial interaction in composite bolted side-plated reinforced-concrete beams", *Structural Engineering and Mechanics*, Vol. 5, No. 5, pp. 553–563.

Roberts, T.M. and Haji-Kazemi, H. (1989). "Strengthening of under-reinforced concrete beams with mechanically attached steel plates", *International Journal of Cement Composites and Lightweight Concrete*, Vol. 11, No. 1, pp. 21–27.

Ruiz, G., Elices, M., and Planas, J. (1999). "Size effect and bond-slip dependence of lightly reinforced concrete beams", In: *European Structural Integrity Society*. Elsevier, pp. 67–97.

Sharif, A., Al-Sulaimani, G.J., Basunbul, I.A., Baluch, M.H., and Husain, M. (1995). "Strengthening of shear-damaged RC beams by external bonding of steel plates", *Magazine of Concrete Research*, Vol. 47, No. 173, pp. 329–334.

Siu, W.H. (2009). *Flexural Strengthening of Reinforced Concrete Beams by Bolted Side Plates*, PhD Thesis, the University of Hong Kong, Hong Kong.

Siu, W.H. and Su, R.K.L. (2009). "Load–deformation prediction for eccentrically loaded bolt groups by a kinematic hardening approach", *Journal of Constructional Steel Research*, Vol. 65, No. 2, pp. 436 – 442.

Siu, W.H. and Su, R.K.L. (2010). "Effects of plastic hinges on partial interaction behaviour of bolted side-plated beams", *Journal of Constructional Steel Research*, Vol. 66, No. 5, pp. 622–633.

Siu, W.H. and Su, R.K.L. (2011). "Analysis of side-plated reinforced concrete beams with partial interaction", *Computers & Concrete*, Vol. 8, No. 1, pp. 71–96.

Su, R.K.L. and Siu, W.H. (2007). "Nonlinear response of bolt groups under in-plane loading", *Engineering structures*, Vol. 29, No. 4, pp. 626–634.

Su, R.K.L., Siu, W.H., and Smith, S.T. (2010). "Effects of bolt-plate arrangements on steel plate strengthened reinforced concrete beams", *Engineering Structures*, Vol. 32, No. 6, pp. 1769–1778.

Su, R.K.L. and Zhu, Y. (2005). "Experimental and numerical studies of external steel plate strengthened reinforced concrete coupling beams", *Engineering structures*, Vol. 27, No. 10, pp. 1537–1550.

NOTATIONS

D_p is the thickness of the steel plates

$(EA)_c$ is the axial stiffness of the unstrengthened RC beam

$(EA)_p$ is the axial stiffness of the steel plates

$(EI)_c$ is the flexural stiffness of the unstrengthened RC beam

$(EI)_p$ is the flexural stiffness of the steel plates

E_p is the Young's modulus of the steel plates

E_s is the Young's modulus of the reinforcement

e_p is the eccentricity of the steel plates relative to the RC beam

F is the load

F_f is the load at failure

F_p is the peak load

f_{co} is the compressive strength of the concrete tested by cylinders

f_{cu} is the compressive strength of the concrete tested by cubes

f_y is the yield stress of the reinforcement

f_{yp} is the yield stress of the steel plates

h_p is the centroidal level of the steel plates

K_e is the equivalent elastic stiffness in the load-deflection curve

k_m is the stiffness of the connecting media

$M_{p,\,b}$ is the bending moment of the steel plates

$M_{p,\,t}$ is the coupling moment of the steel plates $T_p\,e_p$

S_b is the longitudinal bolt spacing

S_{lc} is the longitudinal slip on the steel-concrete interface

S_{tr} is the transverse slip on the steel-concrete interface

T_p is the tension force of the steel plates

U_t is the modulus of toughness

α_ε is the strain factor $\varepsilon_{p,\,hp} / \varepsilon_{p,\,hp}$

α_φ is the curvature factor φ_p / φ_c

β_a is the axial stiffness ratio $(EA)_p / (EA)_c$

β_f is the flexural stiffness ratio $(EI)_p / (EI)_c$

δ_f is the mid-span deflection at failure

δ_p is the mid-span deflection at the peak load

δ_y is the mid-span deflection at the yield point on the equivalent elasto-plastic system

ε_{cc} is the maximum strain on the compression surface of the RC beam

$\varepsilon_{c,\,hp}$ is the strain of the RC beam at the centroidal level of the steel plates

ε_{co} is the crush strain of the concrete

ε_{pc} is the maximum strain on the compressive edge of the steel plates

$\varepsilon_{p,\,hp}$ is the strain of the steel plates at their centroidal level

ε_{pt} is the maximum strain on the tensile edge of the steel plates

ε_{py} is the yield strain of the steel plate

ε_{st} is the strain of the outermost tensile-reinforcement-layer

ε_y is the yield strain of the reinforcement

φ_c is the curvature of the RC beam

φ_p is the curvature of the steel plates

ρ_{st} is the steel ratio of the tensile reinforcement

ρ_{stb} is the balanced tensile steel ratio

Table 1. Concrete material properties and strengthening details

Specimen	f_{cu} (MPa)	f_{co} (MPa)	ρ_{st} (%)	D_p (mm)	S_b (mm)	Rows of bolts	Mid-span bolts	Adhesive in rod-plate clearance	Buckling restraint
Control*	35.2	-	0.85	-	-	-	-	-	-
P75B300	39.7	33.9	0.85	75	300	1	None	None	No
P75B300*	35.3	-	0.85	75	300	1	None	Yes	No
P150B400*	34.6	-	0.85	150	400	2	None	Yes	No
Control	39.1	31.3	1.77	-	-	-	-	-	-
P100B300	33.9	28.9	1.77	100	300	1	Yes	Yes	No
P100B450	40.8	33.2	1.77	100	450	1	Yes	Yes	No
P250B300	36.0	29.7	1.77	250	300	2	Yes	Yes	No
P250B300R	35.8	26.6	1.77	250	300	2	Yes	Yes	Yes
P250B450R	37.7	27.0	1.77	250	450	2	Yes	Yes	Yes

Note: Specimens marked by * were extracted from the experimental study by Siu (2009).

Table 2. Concrete mix proportioning

Water (kg/m^3)	Cement (kg/m^3)	w/c	Fine aggregate (kg/m^3)	Coarse aggregate (kg/m^3)	Maximum aggregate size (mm)	Slump (mm)
200	279	0.72	1025	838	10	50

Table 3. Material properties of reinforcement bars and steel plates

Steel Plates		
Thickness	**f_{yp} (MPa)**	**E_p (GPa)**
6 mm	327	219

Reinforcement bars		
Bar type	**f_y (MPa)**	**E_s (GPa)**
T10	501	211
T16	522	201
R10	298	198

Table 4. Load levels (F/F_p) when failure phenomena occurred

Specimen	(1). Reinforcement tensile yielding $\varepsilon_{st} > \varepsilon_y$	(2). Concrete compressive crushing $\varepsilon_{cc} > \varepsilon_{c0}$	(3). Steel plate tensile yielding $\varepsilon_{pt} > \varepsilon_{py}$	(4). Steel plate compressive buckling $\Delta\varepsilon_{pc} < 0$
P75B300	**0.77**	0.84	0.85	-
Control	**0.91**	0.94	-	-
P100B300	0.87	**0.78**	0.86	-
P100B450	0.85	**0.80**	0.89	-
P250B300	0.88	0.85	**0.26**	**0.96**
P250B300R	0.83	0.84	**0.44**	-
P250B450R	0.83	0.89	**0.29**	-

Table 5. Strength, stiffness and ductility

Specimen	Strength F_p (kN)	Stiffness K_e (kN/mm)	Toughness U_t (kN·mm)
Control*	169.0 (1.00)	9.2 (1.00)	16064 (1.00)
P75B300	222.5 (1.32)	9.4 (1.02)	22264 (1.39)
P75B300*	241.0 (1.43)	10.5 (1.15)	10299 (0.64)
P150B400*	269.2 (1.59)	12.3 (1.34)	10791 (0.67)
Control	267.6 (1.00)	11.5 (1.00)	22915 (1.00)
P100B300	316.9 (1.18)	12.0 (1.04)	18344 (0.80)
P100B450	326.5 (1.22)	12.1 (1.06)	20359 (0.89)
P250B300	359.4 (1.34)	14.6 (1.27)	15021 (0.66)
P250B300R	382.0 (1.43)	14.5 (1.26)	33805 (1.48)
P250B450R	376.7 (1.41)	14.6 (1.27)	31395 (1.37)

Table 6. Summary of slips on the steel-concrete interface

Specimen	Longitudinal slip (mm) at supports		Transverse slip (mm)			
			At supports		At loading points	
	$F/F_p = 0.75$	$F/F_p = 1$	$F/F_p = 0.75$	$F/F_p = 1$	$F/F_p = 0.75$	$F/F_p = 1$
P100B300	0.72	1.50	-0.05	-0.09	0.07	0.30
P100B450	1.12	2.67	-0.06	-0.09	0.12	0.23
P250B300R	0.14	0.29	-0.12	-0.21	0.17	0.46
P250B450R	0.17	0.39	-0.17	-0.33	0.19	0.52

Table 7. Contribution of the steel plates due to bending and tension

Specimen	Tensile force T_p (kN)		Bending moment $M_{p,b}$ (kN·m)		Bending-coupling ratio ($M_{p,b}$ / T_p e_p)	
	$F/F_p = 0.75$	$F/F_p = 1$	$F/F_p = 0.75$	$F/F_p = 1$	$F/F_p = 0.75$	$F/F_p = 1$
P100B300	150 (0.38)	195 (0.50)	2.8	4.6	0.13	0.17
P100B450	144 (0.37)	189 (0.48)	2.9	5.6	0.15	0.20
P250B300R	192 (0.20)	296 (0.30)	42.2	50.8	7.16	6.74
P250B450R	113 (0.12)	196 (0.20)	45.8	54.2	13.08	6.11

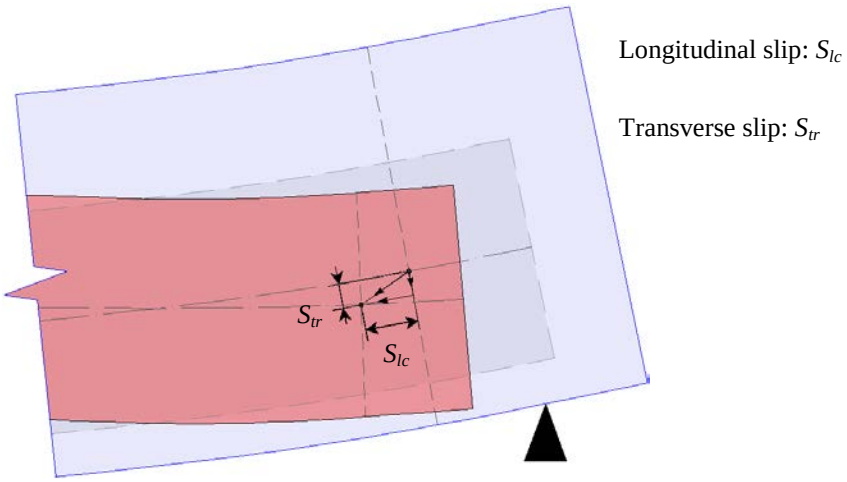

Figure 1. Illustration of longitudinal and transverse slips

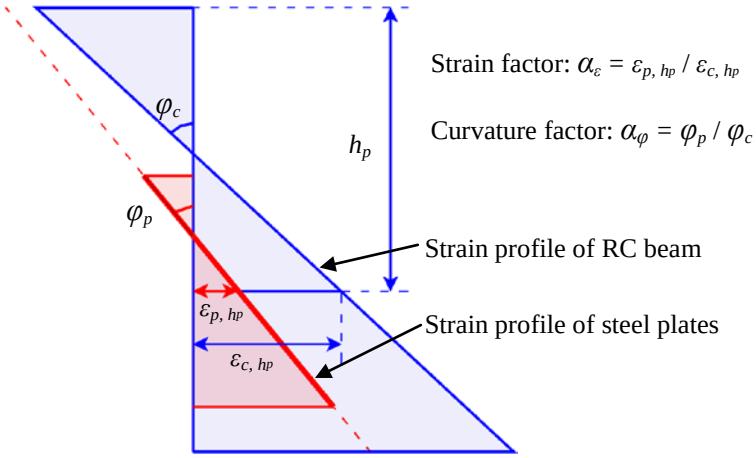

Figure 2. Illustration of strain and curvature factors

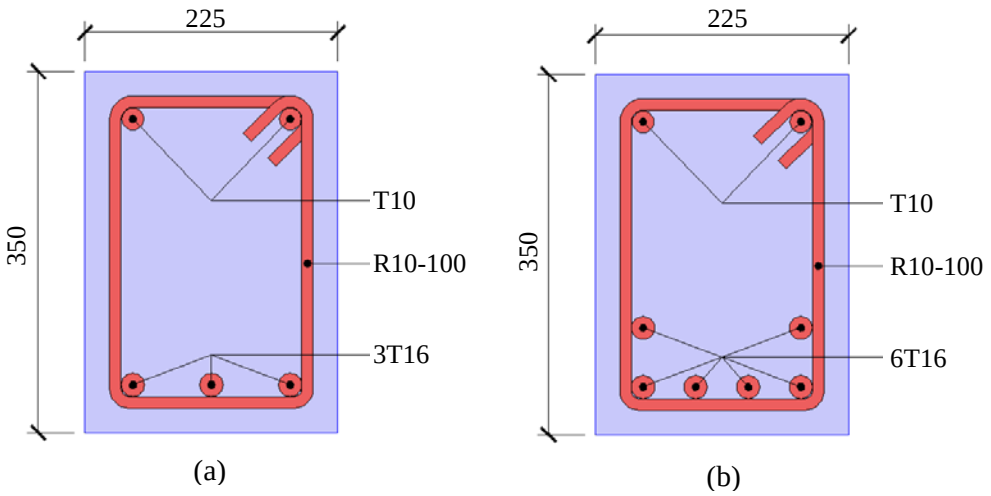

Figure 3. Cross section of specimens that were (a) lightly reinforced and (b) moderately reinforced (dimensions in millimeters)

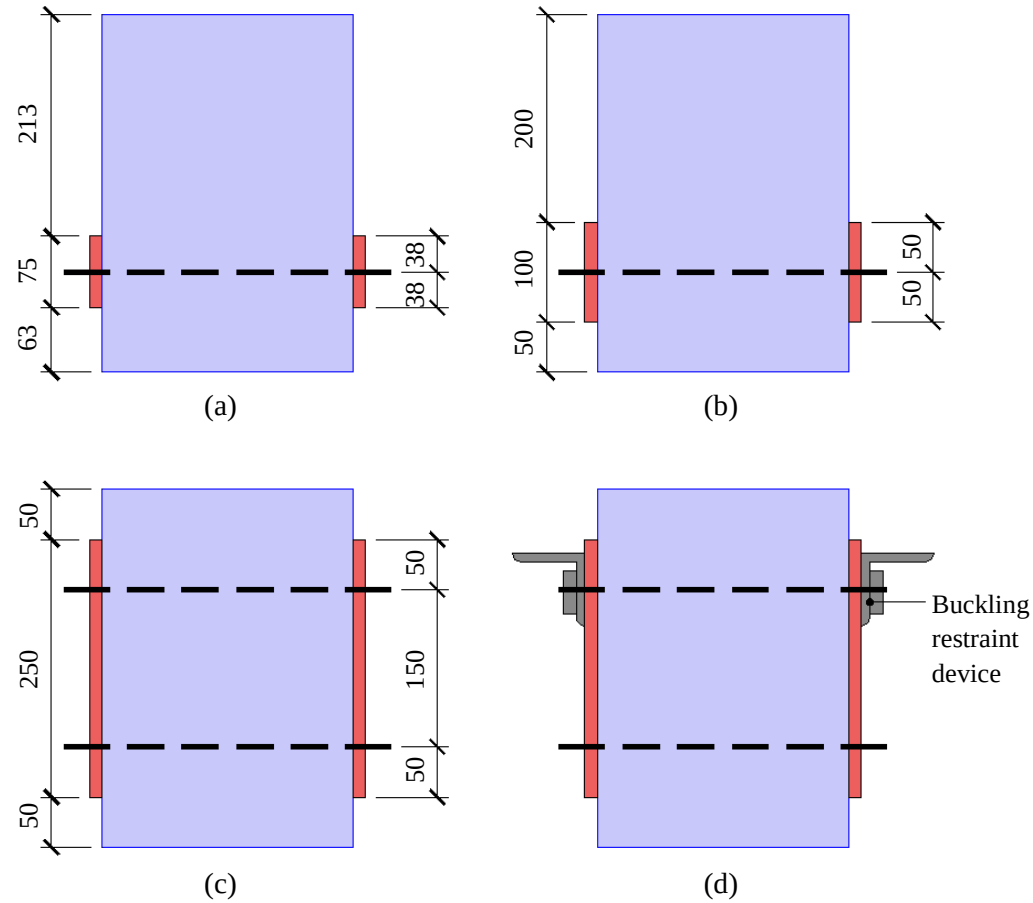

Figure 4. Configurations of strengthening measures (section view) for Specimens (a) P75B300, (b) P100B300 & P100B450, (c) P250B300 and (d) P250B300R & P250B450R (dimensions in millimeters)

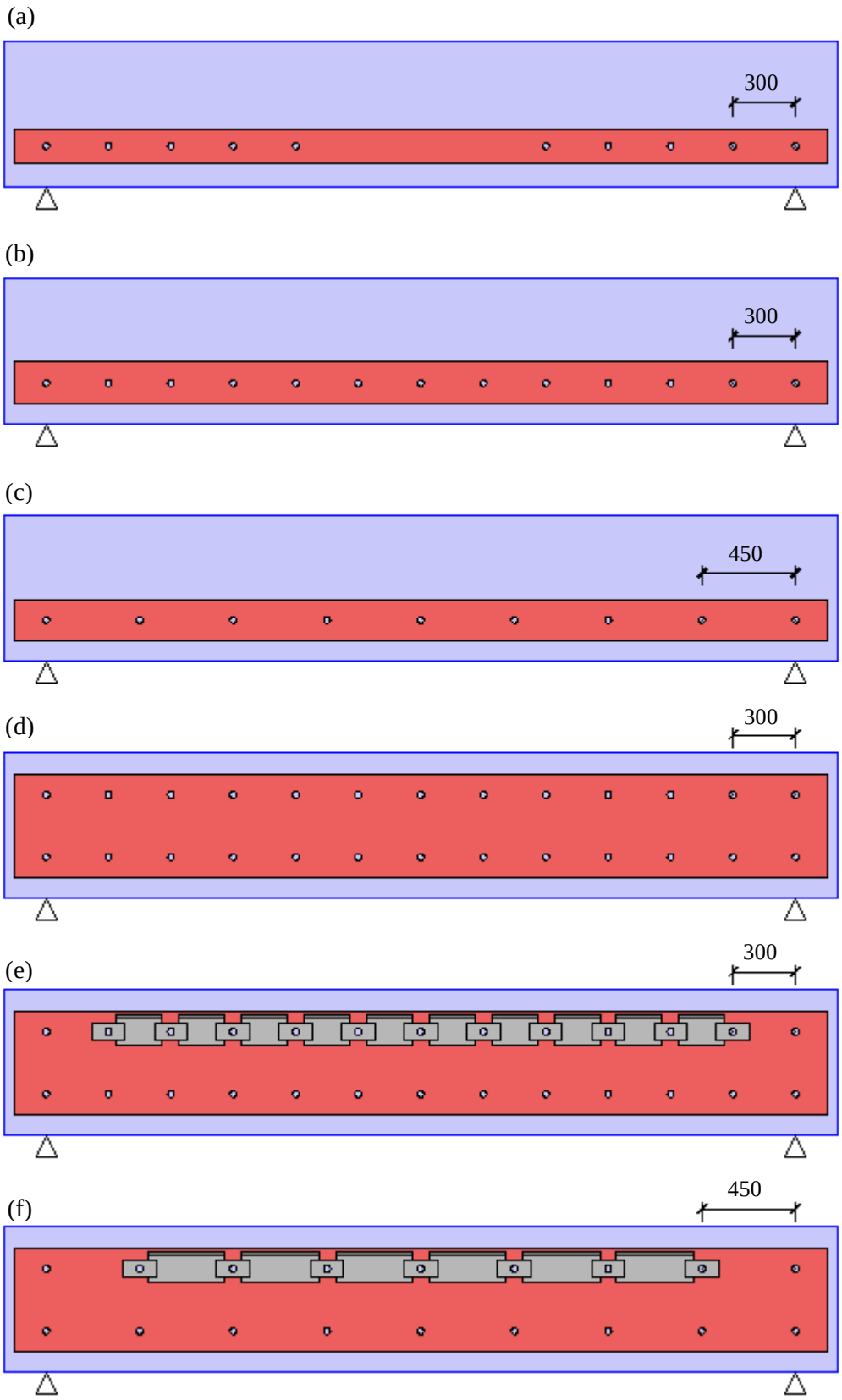

Figure 5. Configurations of strengthening measures (front view) for Specimens (a) P75B300, (b) P100B300, (c) P100B450, (d) P250B300, (e) P250B300R and (f) P250B450R (dimensions in millimeters)

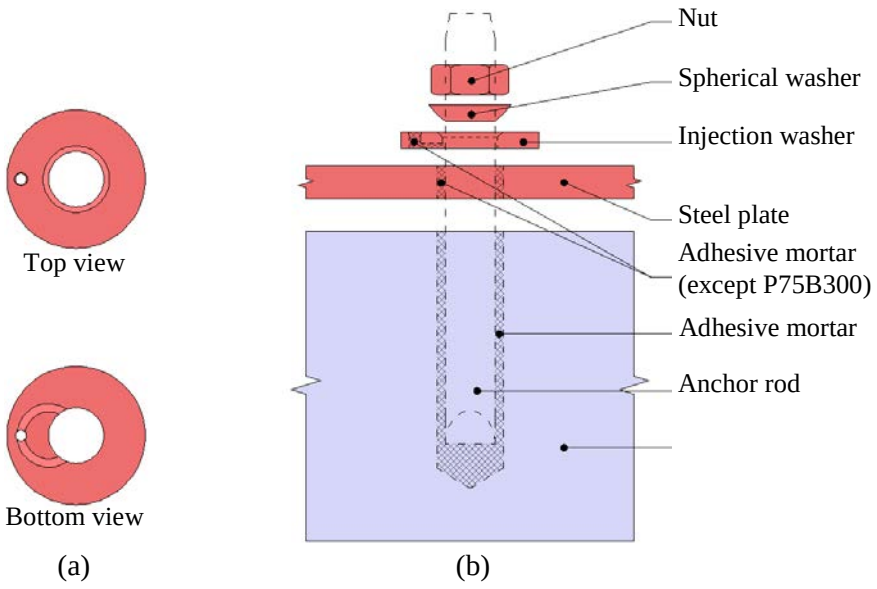

Figure 6. Details and installation of dynamic sets; (a) injection washer and (b) installation drawing

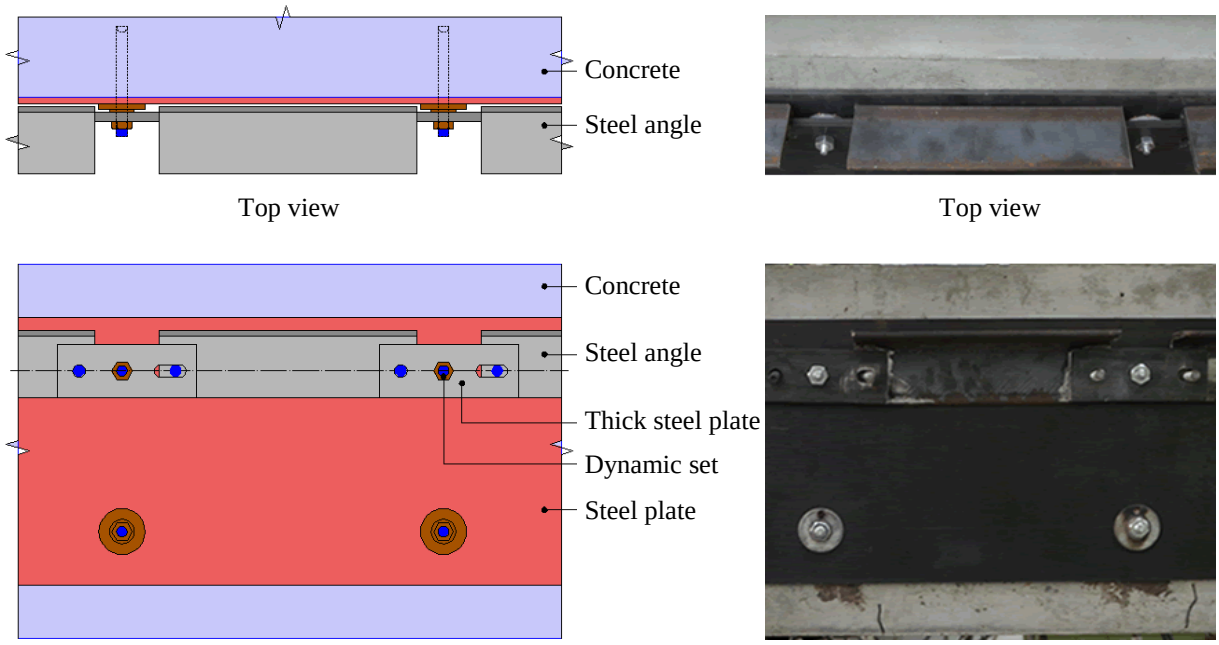

Figure 7. Details and installation of buckling restraint devices; (a) design diagram and (b) actual installation

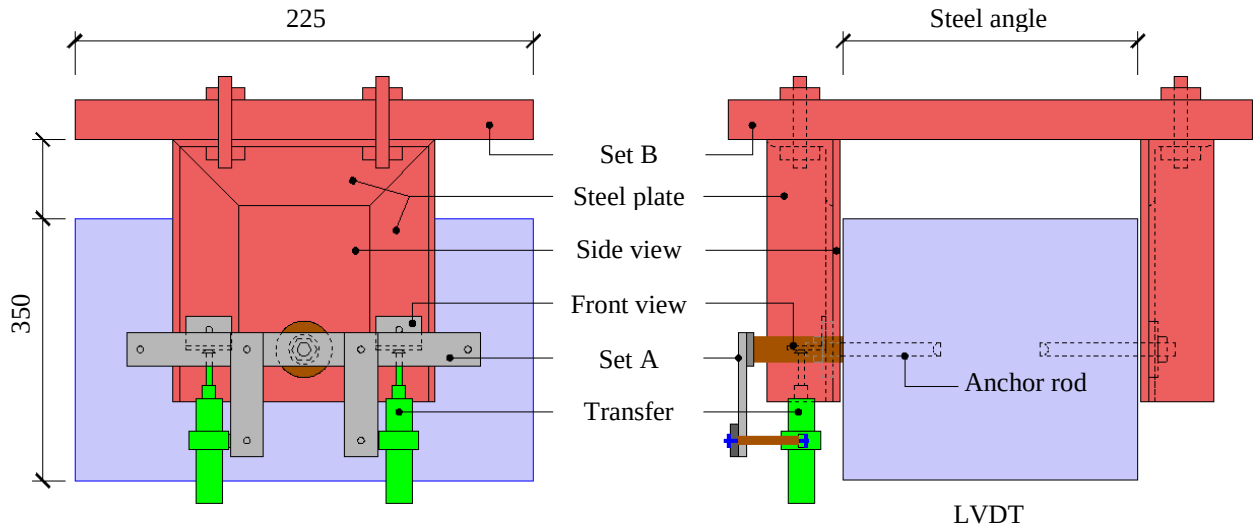

(a)

(b)

Figure 8. Bolt test set-up for the “HIT-RE 500 + HAS-E” anchoring system; (a) design diagram and (b) actual arrangement (dimensions in millimeters)

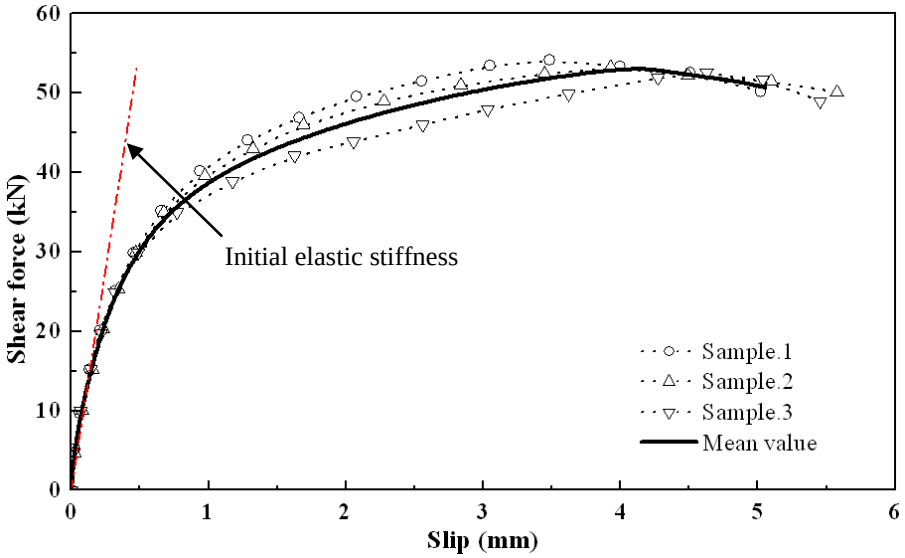

Figure 9. Shear force-slip curves of the "HIT-RE 500 + HAS-E" anchoring system

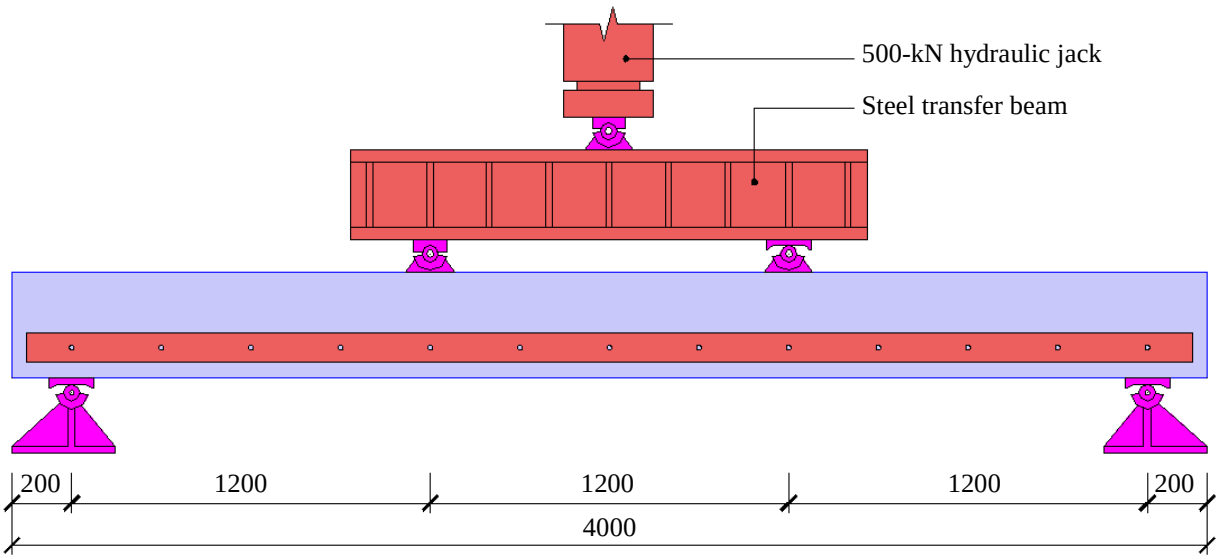

(a)

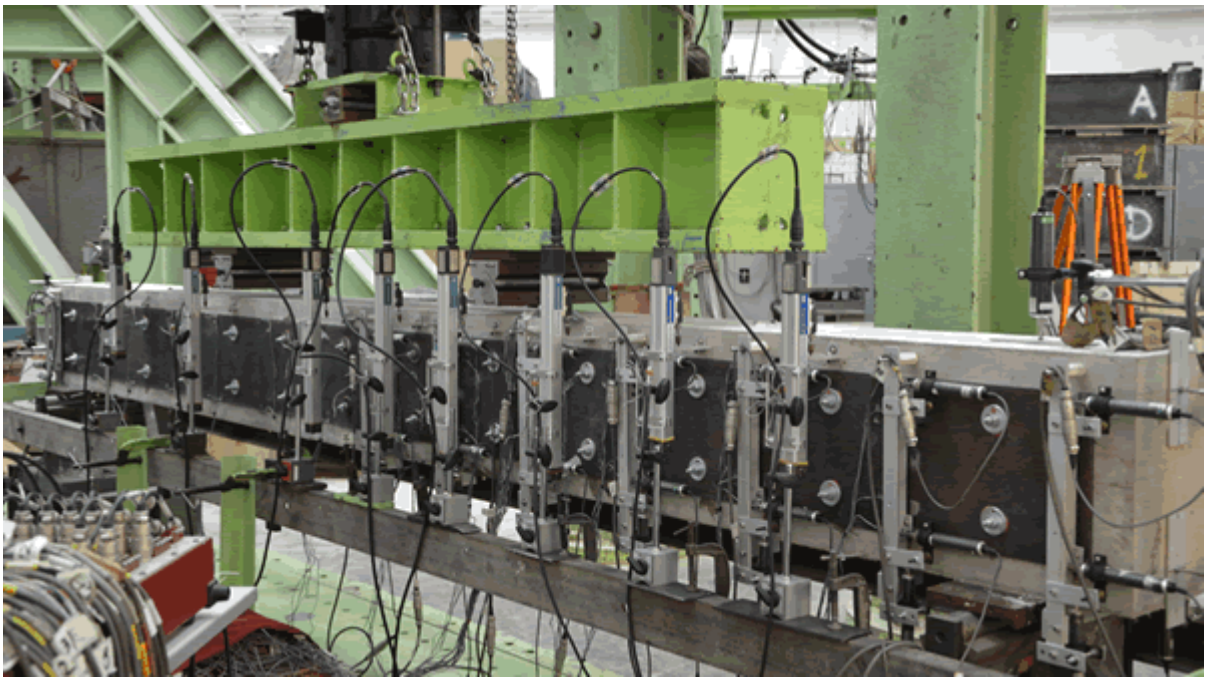

(b)

Figure 10. Test setup; (a) design diagram and (b) actual arrangement (dimensions in millimeters)

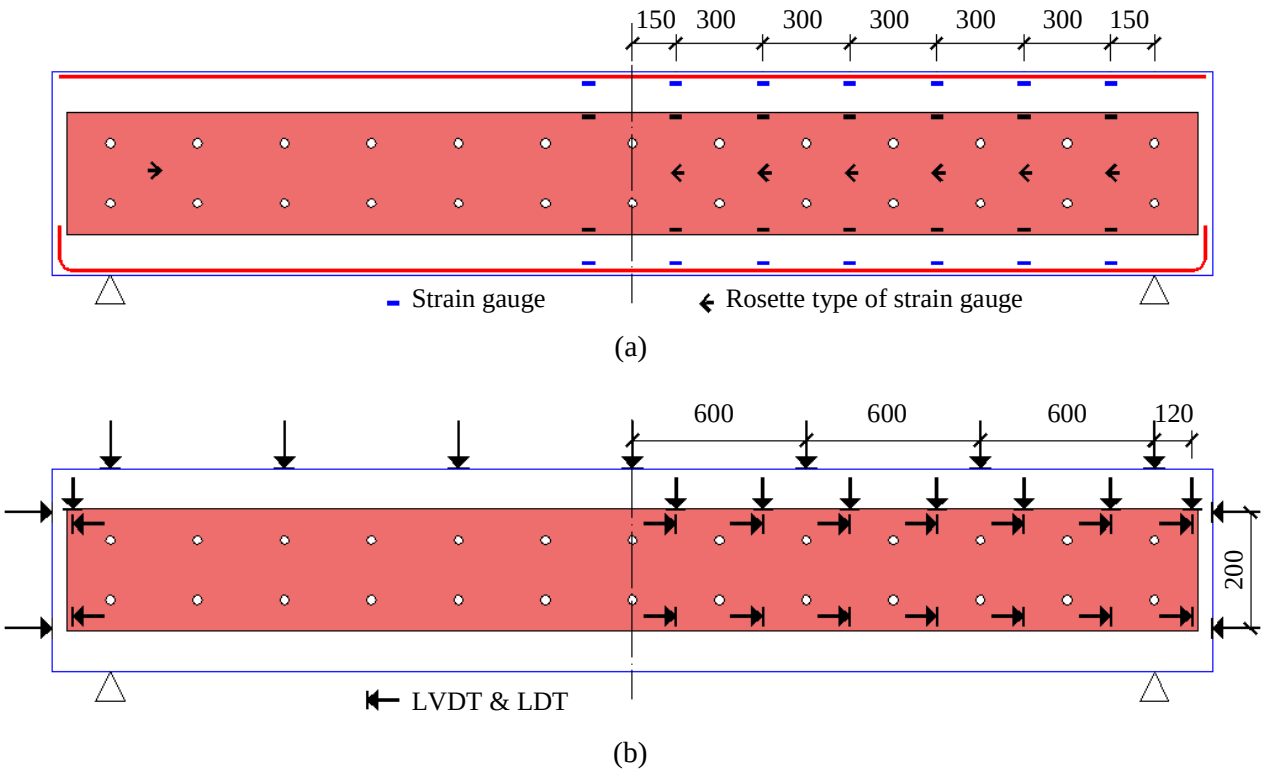

Figure 11. Arrangements of (a) strain gauges and (b) LVDTs & LDTs (dimensions in millimeters)

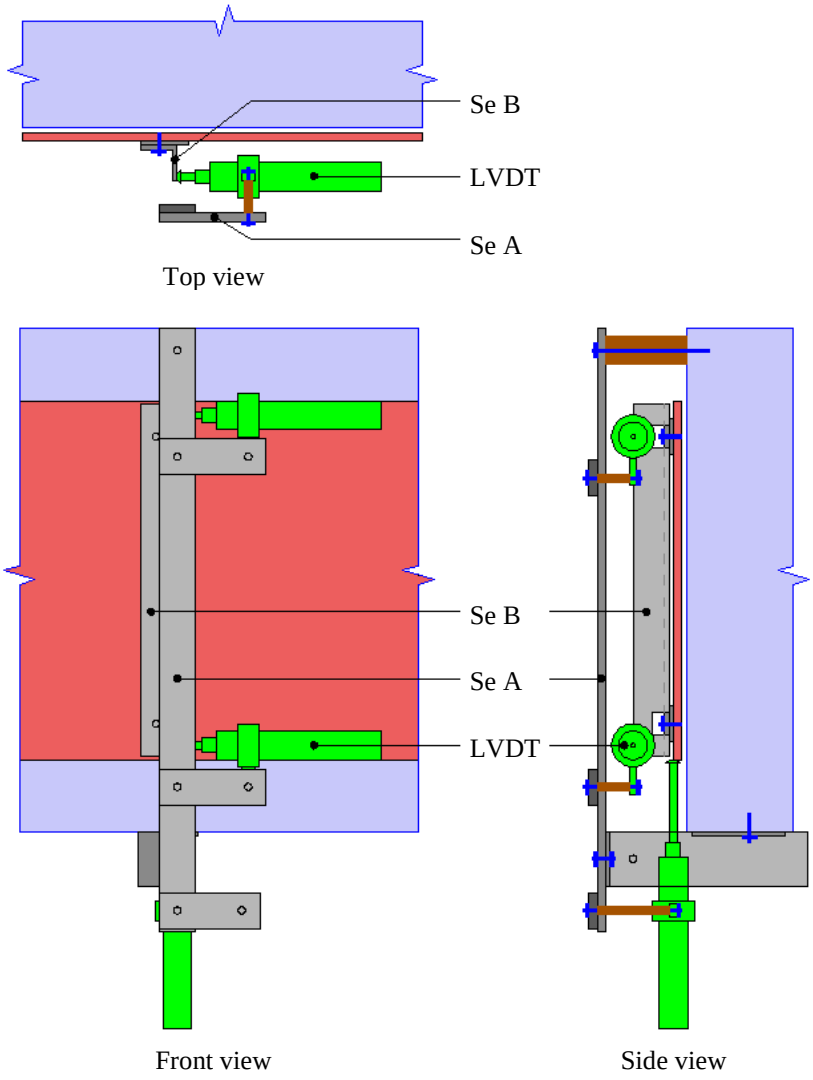

Figure 12. LVDT sets for the measurement of longitudinal and transverse slips

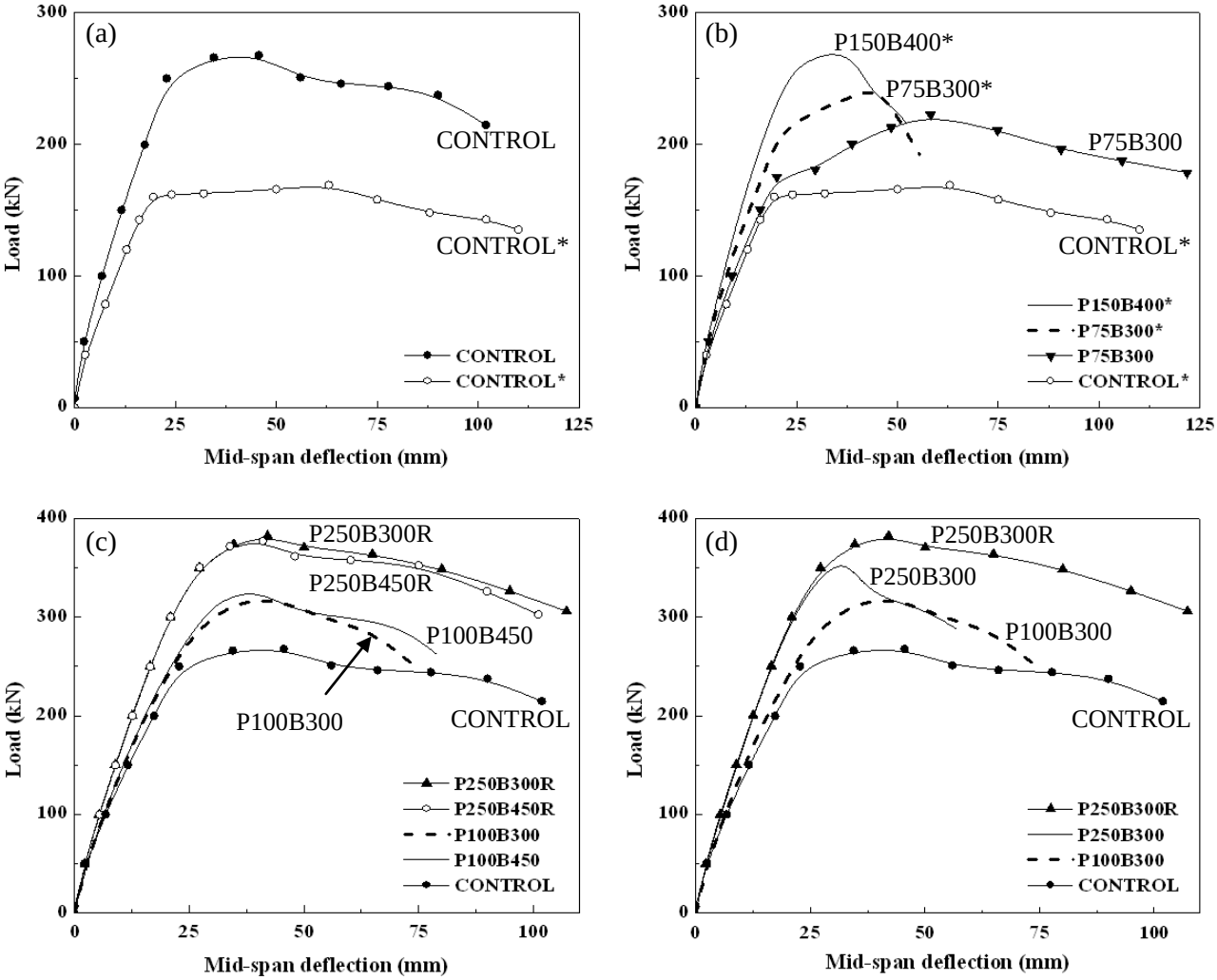

Figure 13. Load-deflection curves for the (a) reference beams, (b) lightly reinforced beams, (c) moderately reinforced beams and (d) beams with or without buckling restraint

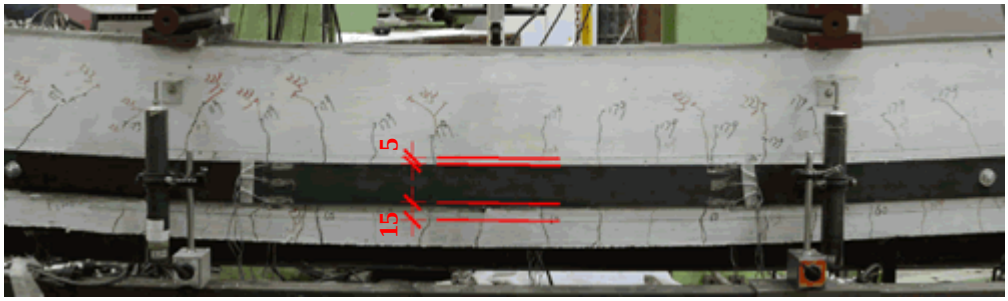

(a)

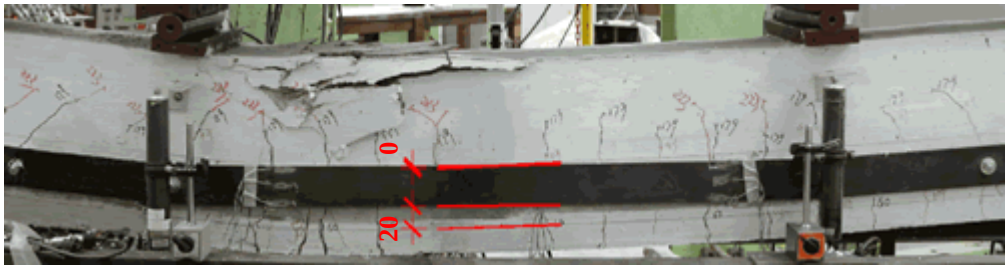

(b)

Figure 14. Mid-span vertical slips of P75B300 at (a) the peak load and (b) failure

(a)

(b)

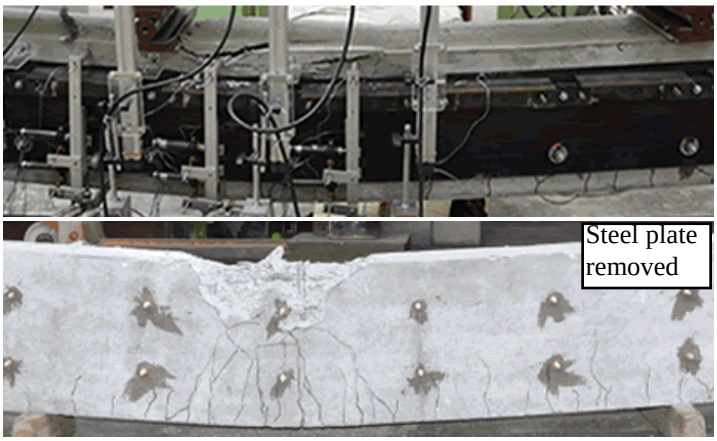

(c)

(d)

Figure 15. Failure modes of Specimens (a) P100B300, (b) P100B450, (c) P250B300R and (d) P250B450R

Figure 16. Plate buckling of Specimen P250B300

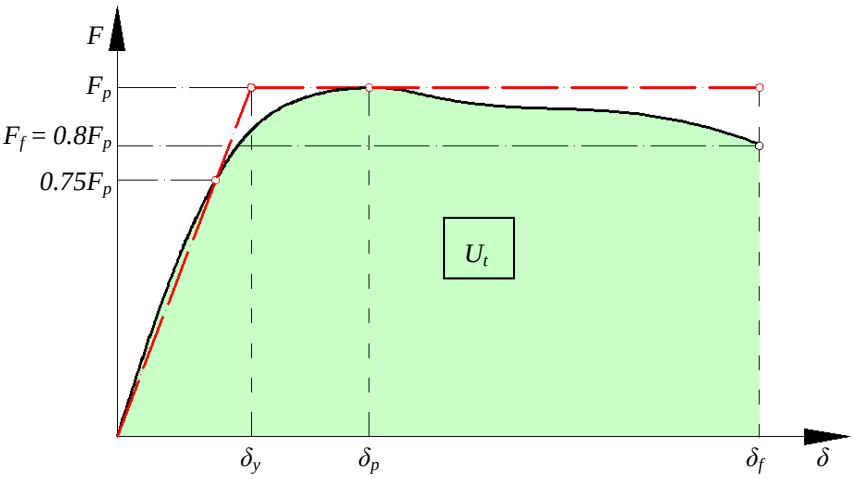

Figure 17. Equivalent elasto-plastic system of the load-deflection curve

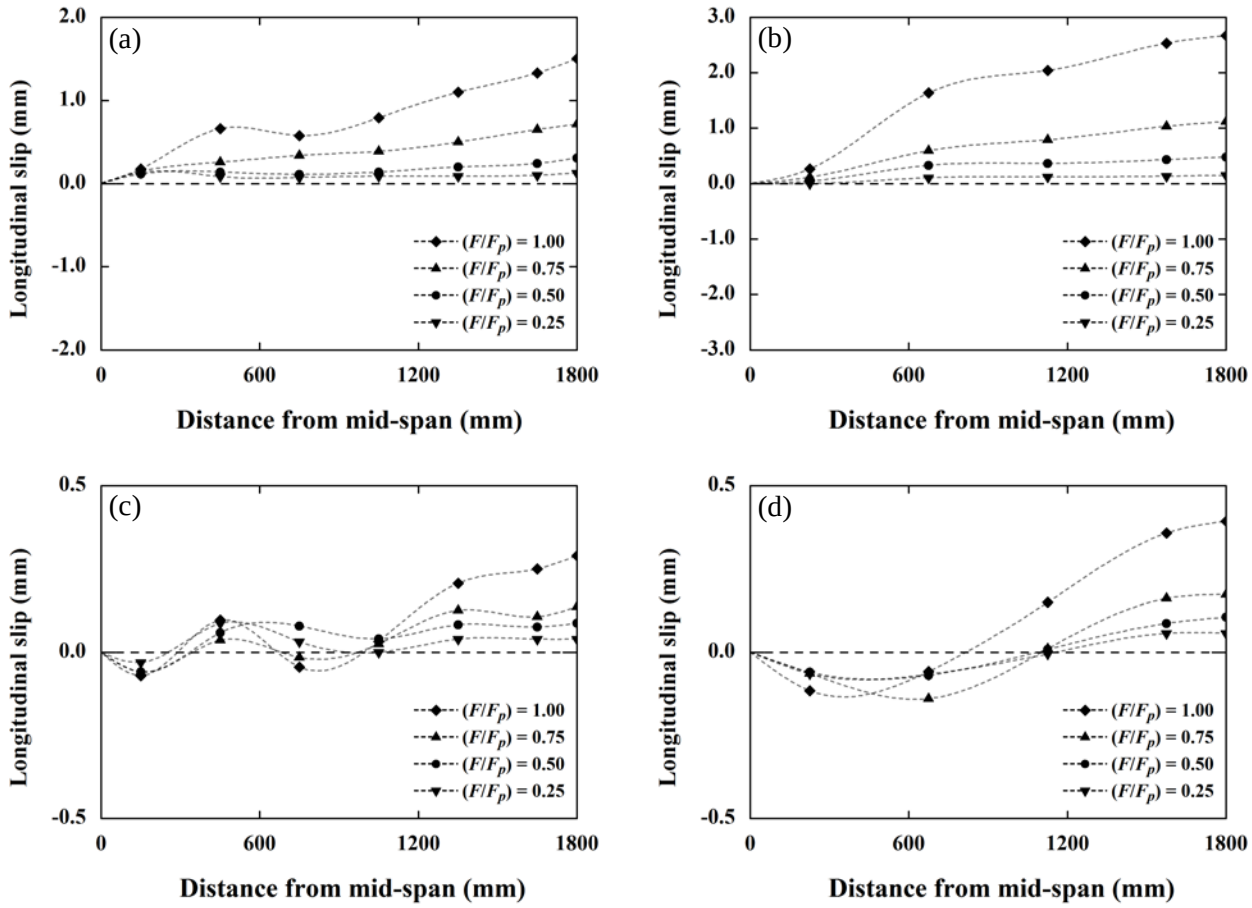

Figure 18. Longitudinal slip distributions along the beam axis for Specimens (a) P100B300, (b) P100B450, (c) P250B300R and (d) P250B450R

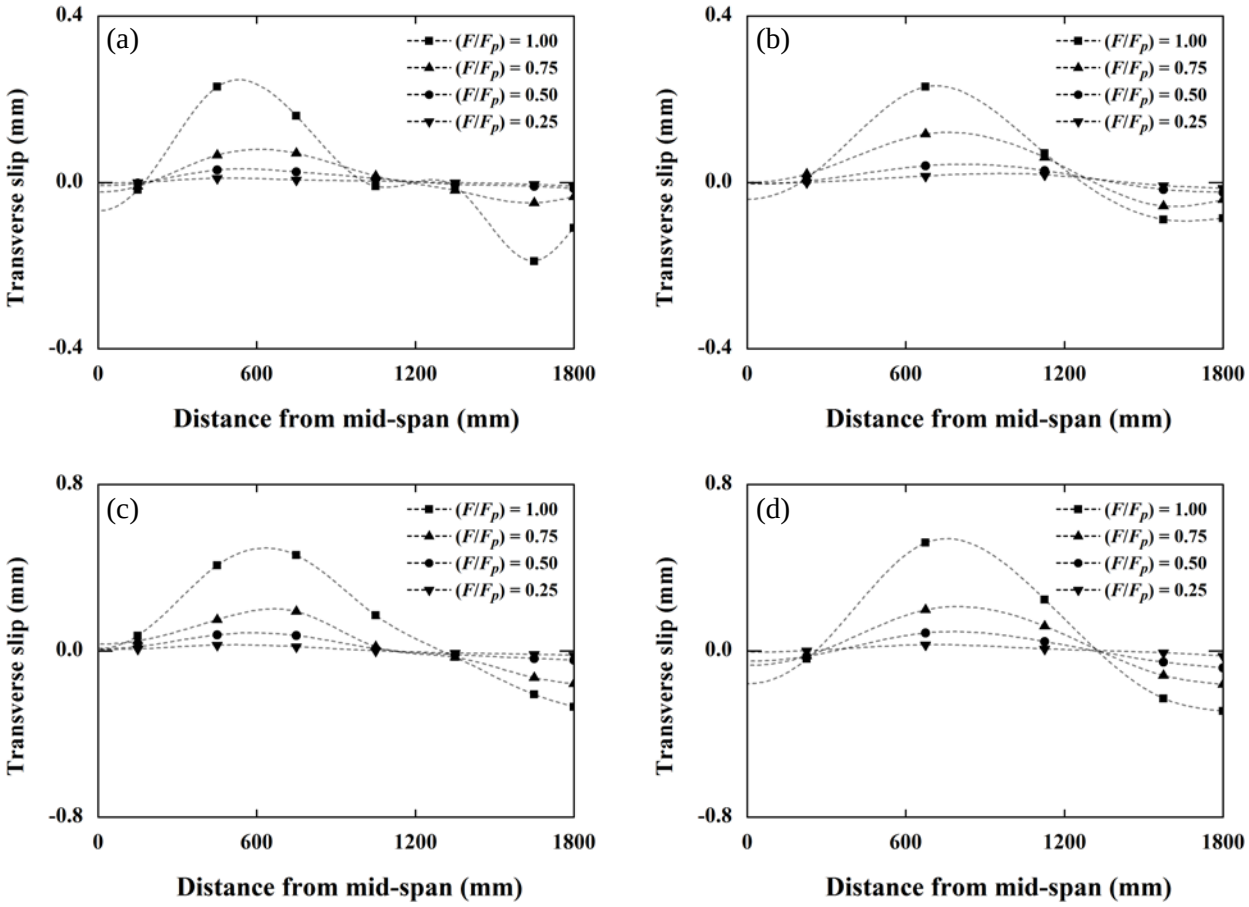

Figure 19. Transverse slip distributions along the beam axis for Specimens (a) P100B300, (b) P100B450, (c) P250B300R and (d) P250B450R

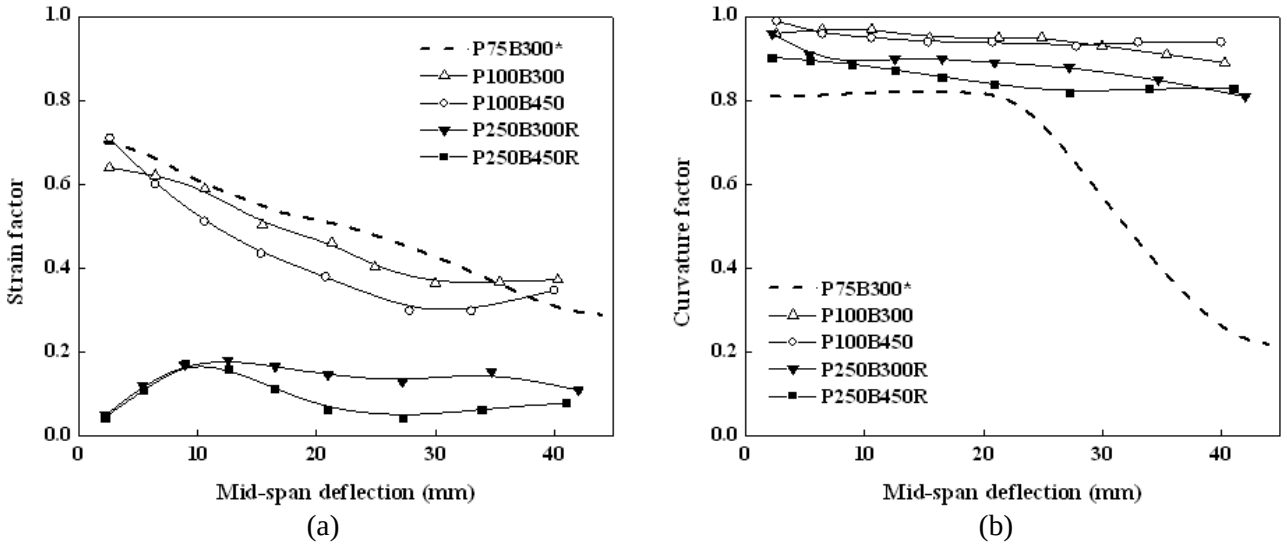

(a) (b)

Figure 20. Development of (a) strain factors and (b) curvature factors